



## UvA-DARE (Digital Academic Repository)

### Frequency Range Selection Method for Vibrational Spectra

Teodoro, T.Q.; Koenis, M.A.J.; Galembeck, S.E.; Nicu, V.P.; Buma, W.J.; Visscher, L.

**DOI**

[10.1021/acs.jpcllett.8b02963](https://doi.org/10.1021/acs.jpcllett.8b02963)

**Publication date**

2018

**Document Version**

Final published version

**Published in**

Journal of Physical Chemistry Letters

**License**

CC BY-NC-ND

[Link to publication](#)

**Citation for published version (APA):**

Teodoro, T. Q., Koenis, M. A. J., Galembeck, S. E., Nicu, V. P., Buma, W. J., & Visscher, L. (2018). Frequency Range Selection Method for Vibrational Spectra. *Journal of Physical Chemistry Letters*, 9(23), 6878-6882. <https://doi.org/10.1021/acs.jpcllett.8b02963>

**General rights**

It is not permitted to download or to forward/distribute the text or part of it without the consent of the author(s) and/or copyright holder(s), other than for strictly personal, individual use, unless the work is under an open content license (like Creative Commons).

**Disclaimer/Complaints regulations**

If you believe that digital publication of certain material infringes any of your rights or (privacy) interests, please let the Library know, stating your reasons. In case of a legitimate complaint, the Library will make the material inaccessible and/or remove it from the website. Please Ask the Library: <https://uba.uva.nl/en/contact>, or a letter to: Library of the University of Amsterdam, Secretariat, Singel 425, 1012 WP Amsterdam, The Netherlands. You will be contacted as soon as possible.

## Frequency Range Selection Method for Vibrational Spectra

T. Q. Teodoro,<sup>†,‡,ⓑ</sup> M. A. J. Koenis,<sup>¶</sup> S. E. Galembeck,<sup>‡,ⓑ</sup> V. P. Nicu,<sup>§</sup> W. J. Buma,<sup>¶</sup> and L. Visscher<sup>\*,†,ⓑ</sup>

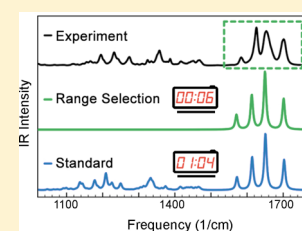
<sup>†</sup>Amsterdam Center for Multiscale Modeling, Faculty of Science, Vrije Universiteit Amsterdam, de Boelelaan 1083, 1081 HV Amsterdam, The Netherlands

<sup>‡</sup>Departamento de Química, FFCLRP, Universidade de São Paulo, Av. Bandeirantes 3900, Ribeirão Preto, 14040-901 São Paulo, Brazil

<sup>¶</sup>Van't Hoff Institute for Molecular Sciences, University of Amsterdam, Science Park 904, 1098 XH Amsterdam, The Netherlands

<sup>§</sup>Department of Environmental Science, Physics, Physical Education and Sport, Lucian Blaga University of Sibiu, Ioan Ratiu Street, Nr. 7-9, 550012 Sibiu, Romania

**ABSTRACT:** Theoretical calculations of vibrational properties are widely used to explain and predict experimental spectra. However, with standard quantum chemical methods all molecular motions are considered, which is rather time-consuming for large molecules. Because typically only a specific spectral region is of experimental interest, we propose here an efficient method that allows calculation of only a selected frequency interval. After a computationally cheap low-level estimate of the molecular motions, the computational time is proportional to the number of normal modes needed to describe this frequency range. Results for a medium-sized molecule show a reduction in computational time of up to 1 order of magnitude with negligible loss in accuracy. We also show that still larger computational savings are possible by using an additional intensity-selection procedure.



The vibrational structure of a molecule can be probed by means of several spectroscopy techniques, such as infrared (IR), Raman, vibrational circular dichroism (VCD), and Raman optical activity (ROA).<sup>1,2</sup> At the core of the methods used to model these properties lies the harmonic approximation to molecular vibrations,<sup>3</sup> which implies the diagonalization of a mass-weighted Hessian

$$\tilde{\mathbf{H}} = \mathbf{M}^{-1/2} \mathbf{H} \mathbf{M}^{-1/2} \quad (1)$$

(with  $\mathbf{M}$  being the atomic mass matrix and the tilde indicating that the Hessian is in mass-weighted coordinates) to obtain as eigenvectors the normal modes,  $\mathbf{U}_i$ , and as eigenvalues the squares of the corresponding fundamental vibrational frequencies,  $\nu_i$ . The computationally intensive task for constructing  $\mathbf{H}$  (the nonmass-weighted Hessian) in eq 1 is to calculate the second derivatives of the molecular energy  $E$  with respect to changes in the nuclear coordinates,  $R_\kappa$  and  $R_\lambda$  (the Greek indices are used in this equation only to represent a general basis for the atomic coordinates):

$$H_{\kappa\lambda} = \frac{d^2 E}{dR_\kappa dR_\lambda} \quad (2)$$

While evaluation of these derivatives is most easily done in Cartesian nuclear coordinates, this approach yields a  $3N_{\text{atoms}} \times 3N_{\text{atoms}}$  dimensional Hessian that is time-consuming to construct in full. Several methods have therefore been proposed to reduce the number of molecular motions that need to be considered explicitly.<sup>4–8</sup> All these methods can be viewed as formally transforming the mass-weighted Hessian in Cartesian coordinates,  $\tilde{\mathbf{H}}^{\text{CC}}$  (where the superscript CC denotes the use of Cartesian coordinates for each of the Hessian

indices), to a  $K$ -dimensional ( $K < 3N_{\text{atoms}}$ ) representation  $\tilde{\mathbf{H}}^{\text{AA}}$  (with the superscript AA referring to use of approximate coordinates for both indices):

$$\tilde{\mathbf{H}}^{\text{AA}} = \mathbf{Q}^{\text{CA}\dagger} \tilde{\mathbf{H}}^{\text{CC}} \mathbf{Q}^{\text{CA}} \quad (3)$$

where  $\mathbf{Q}^{\text{CA}}$  is a rectangular ( $3N_{\text{atoms}} \times K$ ) transformation matrix. The key step is thereby the elimination of motions of molecular fragments that are expected to be less important for interpreting the experimental spectrum (thus  $K$  is equal to number of motions of interest). However, this reduction of the number of coordinates usually relies on the assumption that the normal modes of interest are localized in specific regions of the molecule.

Another approach is the Davidson procedure developed by Reiher and Neugebauer.<sup>9</sup> The method is designed to iteratively refine the normal modes and associated eigenvalues (frequencies) of a set of specific vibrations that are provided as an initial guess. This so-called mode-tracking algorithm is particularly suited to determine local vibrations.<sup>10</sup> For instance, it reproduced in only 20–30% of the computational time the vibrations associated with the thiophenolate anion adsorbed on a Ag(111) surface with the same accuracy as a full vibrational analysis of the whole system.<sup>11</sup>

Here we propose an even simpler “black box” approach in which the iterative refinement stage of the block-Davidson method of ref 9 is omitted entirely. We just compute a full spectrum with a fast approximate method then select and re-

Received: September 26, 2018

Accepted: November 18, 2018

Published: November 19, 2018

evaluate only the normal modes in the spectral interval of experimental interest. This one-step procedure is sufficient if the set of eigenvectors provided by an approximate method spans the space of eigenvectors of the higher-level method in the same spectral interval, which is the case in many practical applications. To sketch the ease of implementation, we will use an index  $j$  for approximate modes, while labeling Cartesian coordinates with the index  $p$ . We start by defining the gradient  $g^C$  of the energy at the target level of theory with respect to nuclear displacements in Cartesian coordinates ( $dR_p^C$ ) as

$$g_p^C = \frac{dE}{dR_p^C} \quad (4)$$

This quantity can be computed analytically in most electronic structure implementations. We then need a second derivative of the energy with respect to the selected set of approximate coordinates. By determining the first-order perturbed wave function with respect to these displacements these matrix elements can in principle also be obtained analytically, but it is easier to use numerical differentiation with an  $n$ -point stencil. For  $n = 2$ , we need  $2K$  displacements along the normal modes of interest calculated at a lower level of theory to obtain a Hessian with one Cartesian and one approximate index,  $\tilde{H}^{CA}$ :

$$\tilde{H}_{pj}^{CA} = \frac{g_p^C(\mathbf{R}^0 + \Delta_j \tilde{\mathbf{R}}_j^A) - g_p^C(\mathbf{R}^0 - \Delta_j \tilde{\mathbf{R}}_j^A)}{2\Delta_j} \quad (5)$$

The displacements  $\Delta_j \tilde{\mathbf{R}}_j^A$  from the equilibrium geometry ( $\mathbf{R}^0$ ) at the target level are taken along the mass-weighted vectors  $\tilde{\mathbf{U}}^{CA} = \mathbf{M}^{-1/2} \mathbf{U}^{CA}$  of the approximate normal modes ( $\mathbf{U}^{CA}$ ) with a step size  $\Delta_j$ . This half-transformed matrix is then further transformed to a square matrix

$$\tilde{\mathbf{H}}^{AA} = (\tilde{\mathbf{U}}^{CA})^\dagger \tilde{\mathbf{H}}^{CA} \quad (6)$$

and it is diagonalized to yield the vibrational frequencies  $\nu_j$  and eigenvectors  $\mathbf{U}^{AR}$  (with AR indicating that this term was obtained on the basis of the approximate modes in the range selection interval). Back transformation of  $\mathbf{U}^{AR}$  provides the normal modes  $\mathbf{U}^{CR}$  expressed in Cartesian coordinates at the target level of theory (with R still referring to the range selection interval):

$$\mathbf{U}^{CR} = \mathbf{U}^{CA} \mathbf{U}^{AR} \quad (7)$$

This representation of the normal modes at the target level of theory is then used to obtain the vibrational spectrum in the selected frequency range. Taking IR as an example, the intensities are straightforwardly obtained in a similar fashion. The  $\mathbf{P}$  tensor of the electric dipole moment derivatives with respect to nuclear displacements (also known as the atomic polar tensor,<sup>12</sup> APT) is thereby constructed via numeric differentiation by calculating electric dipole moment vectors ( $\mu^C$ ) along the approximate modes

$$P_{pj}^{CA} = \frac{\mu_p^C(\mathbf{R}^0 + \Delta_j \tilde{\mathbf{R}}_j^A) - \mu_p^C(\mathbf{R}^0 - \Delta_j \tilde{\mathbf{R}}_j^A)}{2\Delta_j} \quad (8)$$

and then transforming the resulting tensor

$$\mathbf{P}^{CR} = \mathbf{P}^{CA} \mathbf{U}^{AR} \quad (9)$$

Therefore, only energy gradients,  $g_p^C$ , and electric dipole moments,  $\mu_p^C$ , need to be calculated at the target level to provide the IR spectrum of the selected range.

While second derivatives can be calculated at all points on the potential energy surface, including the minima obtained with the approximate method, the harmonic approximation works best if the equilibrium geometry in eq 5 is obtained at the target level of theory. In addition, as is the case in optical properties such as VCD, one may need to compute a number of conformations to obtain proper spectra,<sup>13</sup> which is preferably also done at the higher level of theory to get the best results. Because geometry optimization is, for large systems, much faster than calculation of the Hessian, these steps will not present a computational bottleneck.

The frequency range selection method described above was implemented in a Python-based script for obtaining IR absorption spectra of a pharmaceutical compound, dydrogesterone (Figure 1). Calculations were carried out with the 2017

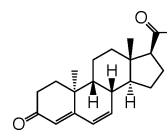
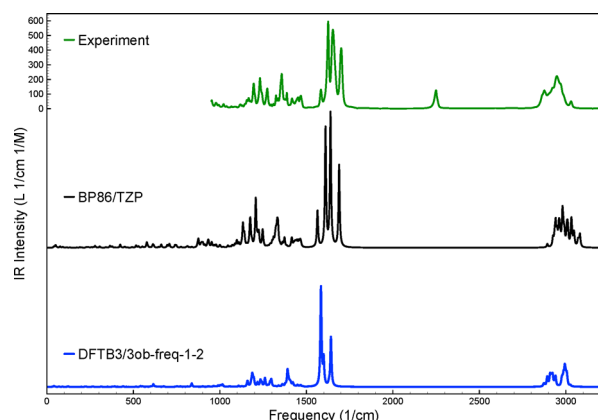


Figure 1. Structure of dydrogesterone.

version of the Amsterdam Density Functional (ADF) modeling suite of programs.<sup>14,15</sup> The target (higher) level was a density functional theory (DFT) method, the Becke–Perdew exchange–correlation potential (BP86),<sup>16–18</sup> in combination with Slater type orbital (STO) nonrelativistic valence triple- $\zeta$  basis sets extended with one polarization function (TZP).<sup>19</sup> The electronic gas-phase ground-state structure obtained at the target level was used in all calculations. The approximate level chosen to provide the normal mode coordinates is a parametrized version of DFT, the third-order density functional-based tight binding method (DFTB3).<sup>20</sup> Parameters for this approximation were taken from the Slater–Koster files for organic and biomolecules, 3ob-freq-1-2.<sup>21</sup> Results were extracted by using the Python Library for Automating Molecular Simulation (PLAMS).<sup>22</sup> Additionally, an experimental spectrum was obtained with dydrogesterone purchased from Sigma-Aldrich with a European Pharmacopoeia Reference standard. A sample of 0.41 M in deuterated chloroform was prepared and injected in a sealed cell with 3 mm thick  $\text{CaF}_2$  windows and a 56  $\mu\text{m}$  sample path length. Subsequently, the Fourier-transform vibrational absorption spectrum was obtained using a Bruker Vertex 70 spectrometer. A baseline correction was performed by using the absorption spectrum of pure deuterated chloroform. All spectra presented in the following were obtained by convoluting calculated stick spectra with a Lorentzian with half width at half-maximum of 4  $\text{cm}^{-1}$ .

As shown in Figure 2, the DFT calculation reproduces the experiment very well. However, a large number of the simulated normal modes are not needed for this comparison as they are not present in the experimental spectrum, viz.,  $\text{CaF}_2$  absorbs below  $\sim 950 \text{ cm}^{-1}$ . Out of the total 153 normal modes computed for this system ( $3 \times 51$  atoms), more than a third (57) belong to this range. Additionally, the bands above 2800  $\text{cm}^{-1}$  in the experimental spectrum, which are associated with C–H stretches, are hardly distinguishable from each other, making the comparison with theory difficult. In the latter range there are 27 calculated bands. By also excluding the 6 rigid



**Figure 2.** Comparison of the experimental (green) IR spectrum of dydrogesterone with spectra calculated at the BP86/TZP (black) and DFTB3/3ob-freq-1-2 (blue) levels. Intensities in the DFTB spectrum were scaled by a factor of 0.3 for better visualization. The experimental band around 2300  $\text{cm}^{-1}$  is not due to dydrogesterone but arises from an experimental artifact due to the solvent.

motions (translations and rotations of the system), only 66 bands distributed in the region from 950 to 1800  $\text{cm}^{-1}$  are actually of interest, which correspond to only 43% of all computed modes.

When using the DFTB3/3ob-freq-1-2 method, computational time was reduced by 2 orders of magnitude with respect to the BP86/TZP calculation. However, as shown in Figure 2, the calculated IR absorption spectrum is quite different than the spectrum calculated at the BP86/TZP level and the experimental spectrum.

In the following, the DFTB3/3ob-freq-1-2 normal mode coordinates are used in the range selection method for the 950–1800  $\text{cm}^{-1}$  interval with BP86/TZP being the target level. The resulting spectrum is shown in Figure 3. The overlap with the full DFT vibrational analysis is nearly perfect even though only 67 modes (44% of the total) were calculated at the same level of theory. In a comparison with the (two-point stencil) numerical evaluation of the full Hessian in a Cartesian basis, the range selection scheme would thus represent a  $\sim 56\%$  reduction in computational time. It has to be noted, however,

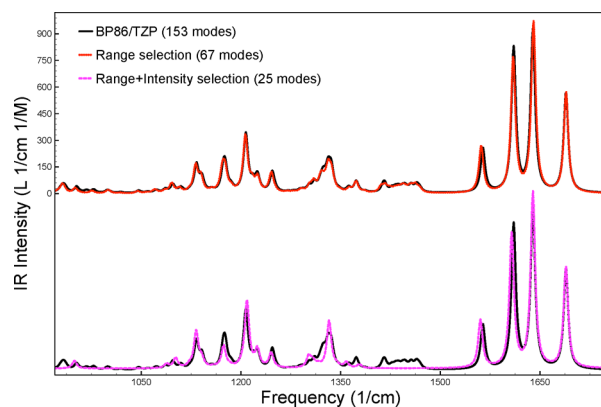


**Figure 3.** Comparison of IR spectra of dydrogesterone in the 950–1800  $\text{cm}^{-1}$  frequency interval calculated at the BP86/TZP level (black), by means of the frequency range selection scheme (red), and with the additional intensity-selection procedure. Only the 25 most intense bands predicted by DFTB3/3ob-freq-1-2 are calculated at the BP86/TZP level (purple).

that analytical Hessian calculations are usually a few times faster than numerical ones with the ADF implementations. With the same computational configuration, the range selection method was about 50% slower than the analytical calculation of the full spectrum.

Therefore, for the present method to be advantageous with respect to the analytical calculation of the full Hessian, a further reduction in the number of modes to be considered is necessary. First, one may additionally screen the modes according to the intensities calculated at the approximate level.<sup>23–25</sup> As Figure 2 shows, although the DFTB bands are not overall reproducing the DFT ones, the ranges where one finds the most intense peaks are fairly similar in both calculations. Thus, we analyzed the outcome of selecting only the most intense bands calculated with the DFTB3/3ob-freq-1-2 model (within the 950–1800  $\text{cm}^{-1}$  frequency range). Results for the intensity selection of 25 bands (16% of the total) are shown in the bottom of Figure 3. Most features of the full DFT spectrum are still reproduced, although this calculation was 40% faster than the analytical evaluation of the full spectrum. Second, one can simply consider a smaller range. In many cases, e.g. in peptides and other large (bio)molecules, one is often interested in only the bands associated with C=O stretching movements. In the dydrogesterone example, there are four very intense bands in the experimental spectrum from  $\sim 1580$  to  $\sim 1700$   $\text{cm}^{-1}$  which are associated with C=O and C=C stretches. To account for this region and deviations in the DFTB frequencies, the range selection scheme was applied in the 1500–1800  $\text{cm}^{-1}$  interval. Results are shown in Figure 4.

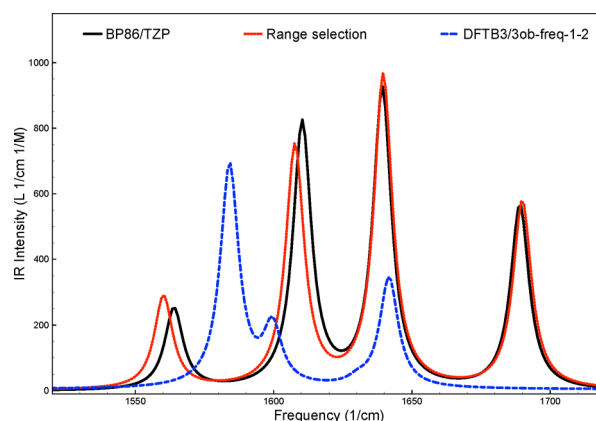


**Figure 4.** Comparison of IR spectra of dydrogesterone calculated at the BP86/TZP (black) and DFTB3/3ob-freq-1-2 (blue) levels and by means of the frequency range selection scheme (red) from 1500 to 1800  $\text{cm}^{-1}$  using normal mode coordinates calculated at the DFTB level. Intensities in the DFTB spectrum were scaled by a factor of 0.3 for better visualization.

The overlap with the BP86/TZP spectrum in the selected range is still very good. One is thus able to obtain virtually the same information with only four normal modes being considered at a high level of theory.

In the example above, a 10 $\times$  reduction in computational time (in comparison with the analytical BP86/TZP calculation of the full spectrum) was achieved. Even larger speed-ups are possible through an analytical implementation.<sup>26</sup> On the other hand, the numerical differentiation exemplified here can be easily parallelized (as already done in the mode-tracking procedure<sup>10</sup>) given that the gradient calculations at each



displaced geometry are independent from each other. We also note in passing that although anharmonic effects are not being addressed in the present analysis, these can be approximately considered by solving one-dimensional Schrödinger equations along each normal mode.<sup>27</sup>

The present method is also expected to perform well for other vibrational properties and larger systems. The example shown next regards the comparison of VCD spectra calculated for a molecule containing a Bucky-ball,  $C_{105}H_{48}O_{18}$ . In this example, the atomic axial tensor (AAT), which appears in the magnetic term in the rotational strength equation,<sup>2</sup> cannot be calculated in the same fashion as the APTs (eq 8), but it can be obtained cheaply at a high level through implementation of the response equations derived by Coriani et al.<sup>28</sup> To illustrate the potential of this approach, the axial tensor and the APT obtained (analytically) with BP86/TZP are applied at all levels shown in the following. As Figure 5 shows, the frequency range

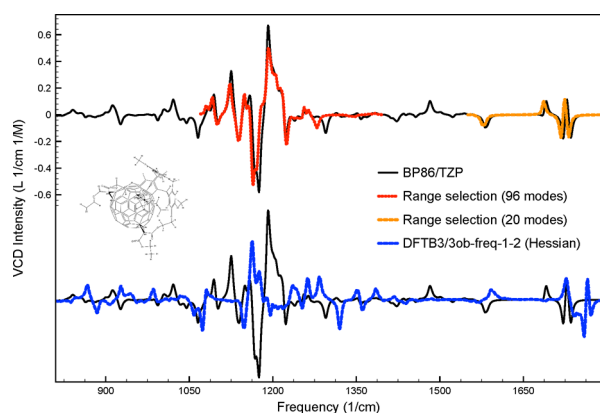


**Figure 5.** Comparison of VCD spectra of  $C_{105}H_{48}O_{18}$  calculated at the BP86/TZP (black) and DFTB3/3ob-freq-1-2 (blue) levels (only in the calculation of the Hessian, as the APT and AAT applied to obtain both spectra were calculated with the DFT level), and by means of the frequency range selection scheme: 1100–1400 (red) and 1700–1800 (orange)  $\text{cm}^{-1}$  using normal mode coordinates calculated at the DFTB level.

selection method (applied in two different regions) yields again spectra that are very comparable with the one from the full analytical BP86/TZP calculation. It is noticeable that even though there are many more near-degenerate modes in certain regions (see the 1100–1400  $\text{cm}^{-1}$  selection) than in the dydrogesterone case, the similarities are still striking. It is also interesting how the present method can cope with very poor modes and frequencies. The comparison in the bottom of Figure 5 shows that even by applying the same APTs and AATs at both (DFT and DFTB) levels, the inaccuracies in the DFTB Hessian yield a completely different spectrum.

One note of caution about the present method can be learned from Figure 5. Even though one of the selections included only the (20) modes predicted by DFTB to be in the 1700–1800  $\text{cm}^{-1}$  range, one notices that the negative band around 1600  $\text{cm}^{-1}$  ends up being described as well. This means that the DFTB frequency of one or some modes was overestimated by more than  $\sim 100 \text{ cm}^{-1}$  with respect to the full BP86/TZP analysis. This appears to be an outlier as overall results are consistent, but it shows that if the lower level yields large deviations in the frequencies, the range selection could be compromised. Hence, the range selection with DFTB and other fast approximate theories, such as semiempirical methods

based on the neglect of differential diatomic overlap integral approximation,<sup>29,30</sup> should take into account the expected error margin for such methods.

In conclusion, the range selection method outlined here is shown to be a powerful tool for obtaining accurate vibrational spectra of a selected frequency interval. As the computational effort is limited to the number of normal modes within the region, this method will be particularly interesting for large molecules (e.g., proteins) for which only a handful of modes out of thousands, such as amide carbonyl stretches<sup>31</sup> or low-lying modes,<sup>32</sup> are of interest.

## AUTHOR INFORMATION

### Corresponding Author

\*E-mail: l.visscher@vu.nl

### ORCID

T. Q. Teodoro: 0000-0003-4590-0056

S. E. Galembeck: 0000-0001-5018-4643

L. Visscher: 0000-0002-7748-6243

### Notes

The authors declare no competing financial interest.

## ACKNOWLEDGMENTS

This research received funding from The Netherlands Organisation for Scientific Research in the framework of the Fund New Chemical Innovations (NWO Project Nr. 731.014.209). T.Q.T. thanks the São Paulo Research Foundation (FAPESP Projects Nr. 2016/07787-4 and 2016/23165-3) for a postdoctoral grant. S.E.G. also acknowledges FAPESP (Projects Nr. 2008/02677-0 and 2014/50265-3) and the National Council for Scientific and Technological Development (CNPq Project Nr. 308254/2016-3). We also thank Dr. R. Rüger, M.Sc. M. Handzlik, and Dr. S. van Gisbergen for useful discussions.

## REFERENCES

- (1) Wilson, E., Jr.; Decius, J.; Cross, P. *Molecular Vibrations: The Theory of Infrared and Raman Vibrational Spectra*; Dover Publications, Inc.: New York, 1955.
- (2) Barron, L. D.; Buckingham, A. D. Vibrational optical activity. *Chem. Phys. Lett.* **2010**, *492*, 199–213.
- (3) Woodward, L. *Molecular Vibrations and Vibrational Spectroscopy*; Oxford University Press: Oxford, U.K., 1972.
- (4) Li, H.; Jensen, J. H. Partial Hessian vibrational analysis: the localization of the molecular vibrational energy and entropy. *Theor. Chem. Acc.* **2002**, *107*, 211–219.
- (5) Ghysels, A.; Van Neck, D.; Van Speybroeck, V.; Verstraelen, T.; Waroquier, M. Vibrational modes in partially optimized molecular systems. *J. Chem. Phys.* **2007**, *126*, 224102.
- (6) Jacob, C. R.; Reiher, M. Localizing normal modes in large molecules. *J. Chem. Phys.* **2009**, *130*, 084106.
- (7) Woodcock, H. L.; Zheng, W.; Ghysels, A.; Shao, Y.; Kong, J.; Brooks, B. R. Vibrational subsystem analysis: A method for probing free energies and correlations in the harmonic limit. *J. Chem. Phys.* **2008**, *129*, 214109.
- (8) Ghysels, A.; Van Speybroeck, V.; Pauwels, E.; Catak, S.; Brooks, B. R.; Van Neck, D.; Waroquier, M. Comparative study of various normal mode analysis techniques based on partial Hessians. *J. Comput. Chem.* **2009**, *31*, 994–1007.
- (9) Reiher, M.; Neugebauer, J. A mode-selective quantum chemical method for tracking molecular vibrations applied to functionalized carbon nanotubes. *J. Chem. Phys.* **2003**, *118*, 1634–1641.

- (10) Herrmann, C.; Neugebauer, J.; Reiher, M. Finding a needle in a haystack: direct determination of vibrational signatures in complex systems. *New J. Chem.* **2007**, *31*, 818–831.
- (11) Herrmann, C.; Reiher, M. Direct targeting of adsorbate vibrations with mode-tracking. *Surf. Sci.* **2006**, *600*, 1891–1900.
- (12) Person, W. B.; Newton, J. H. Dipole moment derivatives and infrared intensities. I. Polar tensors. *J. Chem. Phys.* **1974**, *61*, 1040–1049.
- (13) Heshmat, M.; Nicu, V. P.; Baerends, E. J. On the Equivalence of Conformational and Enantiomeric Changes of Atomic Configuration for Vibrational Circular Dichroism Signs. *J. Phys. Chem. A* **2012**, *116*, 3454–3464.
- (14) Baerends, E. J.; Ziegler, T.; Atkins, A. J.; Autschbach, J.; Bashford, D.; Baseggio, O.; Bérces, A.; Bickelhaupt, F. M.; Bo, C.; Boerrigter, P. M. et al. ADF2017, SCM, *Theoretical Chemistry*; Vrije Universiteit: Amsterdam, The Netherlands; <https://www.scm.com> (accessed November 13, 2018).
- (15) te Velde, G.; Bickelhaupt, F. M.; Baerends, E. J.; Fonseca Guerra, C.; van Gisbergen, S. J. A.; Snijders, J. G.; Ziegler, T. Chemistry with ADF. *J. Comput. Chem.* **2001**, *22*, 931–967.
- (16) Becke, A. D. Density-functional exchange-energy approximation with correct asymptotic behavior. *Phys. Rev. A: At, Mol, Opt. Phys.* **1988**, *38*, 3098–3100.
- (17) Perdew, J. P. Density-functional approximation for the correlation energy of the inhomogeneous electron gas. *Phys. Rev. B: Condens. Matter Mater. Phys.* **1986**, *33*, 8822–8824.
- (18) Perdew, J. P. Erratum: Density-functional approximation for the correlation energy of the inhomogeneous electron gas. *Phys. Rev. B: Condens. Matter Mater. Phys.* **1986**, *34*, 7406–7407.
- (19) Van Lenthe, E.; Baerends, E. J. Optimized Slater-type basis sets for the elements 1–118. *J. Comput. Chem.* **2003**, *24*, 1142–1156.
- (20) Gaus, M.; Cui, Q.; Elstner, M. DFTB3: Extension of the Self-Consistent-Charge Density-Functional Tight-Binding Method (SCC-DFTB). *J. Chem. Theory Comput.* **2011**, *7*, 931–948.
- (21) Gaus, M.; Goez, A.; Elstner, M. Parametrization and benchmark of DFTB3 for organic molecules. *J. Chem. Theory Comput.* **2013**, *9*, 338–354.
- (22) Handzlik, M. Python Library for Automating Molecular Simulation, PLAMS, 2018; <https://github.com/SCM-NV/PLAMS> (accessed November 13, 2018).
- (23) Luber, S.; Neugebauer, J.; Reiher, M. Intensity tracking for theoretical infrared spectroscopy of large molecules. *J. Chem. Phys.* **2009**, *130*, 064105.
- (24) Kiewisch, K.; Neugebauer, J.; Reiher, M. Selective calculation of high-intensity vibrations in molecular resonance Raman spectra. *J. Chem. Phys.* **2008**, *129*, 204103.
- (25) Rügner, R.; van Lenthe, E.; Lu, Y.; Frenzel, J.; Heine, T.; Visscher, L. Efficient calculation of electronic absorption spectra by means of intensity-selected Time-Dependent Density Functional Tight Binding. *J. Chem. Theory Comput.* **2015**, *11*, 157–167.
- (26) Ghysels, A.; Woodcock, H. L.; Larkin, J. D.; Miller, B. T.; Shao, Y.; Kong, J.; Neck, D. V.; Speybroeck, V. V.; Waroquier, M.; Brooks, B. R. Efficient Calculation of QM/MM Frequencies with the Mobile Block Hessian. *J. Chem. Theory Comput.* **2011**, *7*, 496–514.
- (27) Piccini, G.; Sauer, J. Quantum chemical free energies: structure optimization and vibrational frequencies in normal modes. *J. Chem. Theory Comput.* **2013**, *9*, 5038–5045.
- (28) Coriani, S.; Thorvaldsen, A. J.; Kristensen, K.; Jorgensen, P. Variational response-function formulation of vibrational circular dichroism. *Phys. Chem. Chem. Phys.* **2011**, *13*, 4224–4229.
- (29) Pople, J. A.; Santry, D. P.; Segal, G. A. Approximate self-consistent molecular orbital theory. I. Invariant procedures. *J. Chem. Phys.* **1965**, *43*, S129–S135.
- (30) Pople, J. A.; Beveridge, D. L.; Dobosh, P. A. Approximate Self-Consistent Molecular-Orbital Theory. V. Intermediate Neglect of Differential Overlap. *J. Chem. Phys.* **1967**, *47*, 2026–2033.
- (31) Kubelka, J.; Keiderling, T. A. Ab Initio calculation of amide carbonyl stretch vibrational frequencies in solution with modified basis sets. I. N-methyl acetamide. *J. Phys. Chem. A* **2001**, *105*, 10922–10928.
- (32) Ghysels, A.; Van Speybroeck, V.; Pauwels, E.; Van Neck, D.; Brooks, B. R.; Waroquier, M. Mobile Block Hessian Approach with adjoined blocks: An efficient approach for the calculation of frequencies in macromolecules. *J. Chem. Theory Comput.* **2009**, *5*, 1203–1215.